

Current Distribution in the Three-Dimensional Random Resistor Network at the Percolation Threshold

G. George Batrouni

HLRZ Forschungszentrum, D-52425 Jülich, Germany

Alex Hansen

Institutt for fysikk, Norges tekniske høyskole, N-7034 Trondheim, Norway

Brond Larson*

Thinking Machines Corporation, 245 First Street, Cambridge MA 02142, USA

(September 26, 2018)

Abstract

We study the multifractal properties of the current distribution of the three-dimensional random resistor network at the percolation threshold. For lattices ranging in size from 8^3 to 80^3 we measure the second, fourth and sixth moments of the current distribution, finding *e.g.* that $t/\nu = 2.282(5)$ where t is the conductivity exponent and ν is the correlation length exponent.

PACS numbers: 64.40.Ak, 72.20.-i, 72.70+m, 05.40.+j

Typeset using REVTeX

*Current address: Silicon Graphics Computer Systems, 1 Cabot Road, Hudson, MA 01749, USA.

I. INTRODUCTION

Quite surprisingly, it was found in the mid-eighties that dynamic phenomena on fractal structures often were controlled not by one or two relevant length scales, but rather an infinite hierarchy of such length scales [1]. One of the prime examples of this phenomenon is the current distribution in the random resistor network at the percolation threshold [2–5]. In spite of the large effort which was invested to understand how such an infinite hierarchy could appear, *e.g.* through studying hierarchical structures yielding to analytic calculations [3,5], no satisfactory general explanation was found. The large numerical effort that was invested at that time on the random resistor network focussed on two dimensions. The reason for this was that three-dimensional networks were essentially out of reach of the computational power available at the time. The aim of the present work is to establish that, as in two dimensions, the current distribution in three dimensions is multifractal and to determine the corresponding scaling exponents with high precision. In addition to their theoretical interest, these results are of importance in making contact with experimental studies on three-dimensional conductor-insulator mixtures [6–8], and microemulsions [9–13]. To achieve this goal, we made use of the latest developments in iterative solvers and massively parallel computers.

In section II we present the model and the method of solution. In section III we discuss the current distribution through the behaviour of the moments and their exponents, in addition to examining the statistical fluctuations of the moments.

II. MODEL AND NUMERICAL SOLUTION

We consider a three-dimensional cubic lattice of size L^3 with periodic boundary conditions in the x and y directions. For the z direction the boundary conditions are as follows: At $z = 1$ and $z = L$ we place two plates with a constant potential difference set at a value of 1. Therefore, the length of the lattice in the z direction is $(L - 1)$, while in the x and

y directions the length is L . This geometry was chosen because the data layout becomes optimal on the Connection Machine CM5 which we used for our computations.

All bonds are visited and, with a probability p , a resistor is placed. All resistors have the same resistance, 1. We set p equal to the bond percolation threshold for the cubic lattice, $p_c = 0.2488$, as determined by Stauffer *et al.* [14]. After all the bonds have been visited, a (parallel) cluster finding algorithm is applied to determine if there is a spanning cluster that connects the two plates. If no such cluster exists, the procedure is repeated until one is obtained. This cluster finding algorithm is very fast but only determines if there is such a cluster, not its exact geometry.

The equations to be solved are the usual current equations (Kirchhoff's equations) on the lattice which can be easily solved using the conjugate gradient or related iterative algorithms [15]. We wrote the program in CM Fortran and used the iterative solvers in the Connection Machine Scientific Software Library (CMSSL) which contains thirteen of them. Which one to use, depends on the particular matrices one is dealing with. For this problem we found that the quasi-minimized CGS (QCGS) [16] algorithm performs very well.

Our stopping condition is for the residual to be less than 10^{-12} , which for the biggest lattices gave a true accuracy of about 10^{-9} . We estimated this by calculating the conductivity of each realization in two ways: 1) Calculate the total current crossing an XY plane at $z = L/2$, which, knowing the potential difference ($=1$), gives the conductivity, and 2) calculate the second moment of the currents. This is again equal the conductivity as the externally applied potential difference is 1. On the biggest lattices, for which the accuracy at which we can determine the currents is the lowest, they agreed to within $O(10^{-9})$. As it is too time consuming compared to solving the Kirchhoff equations, we made no effort to identify the bonds that did not belong to the spanning cluster. We simply solved for the currents keeping the disconnected bonds and dangling ends in the system. This made it impossible to get an accurate count of the number of current-carrying bonds. We will, therefore, give results for the second, fourth, and sixth moments of the currents, leaving out the zero'th moment. The number of realizations for $L = 8, 16, 32, 48, 64,$ and 80 were

12000, 9198, 2765, 1120, 1913, and 953 respectively.

III. CURRENT DISTRIBUTION

Solving for the currents in the bonds allows us to calculate the n th moment of the current distribution, given by

$$\langle i^n \rangle_V = \frac{1}{N_R} \sum_R \sum_{k(R)} i_{k(R)}^n, \quad (1)$$

where R denotes the realization, N_R is the number of these realizations, and $i_{k(R)}$ is the current in the k th bond in realization R . These moments are calculated in the constant voltage ensemble where the potential difference is kept constant realization to realization. We expect the moments of the currents to scale as

$$\langle i^n \rangle_V \sim L_z^{x(n)}, \quad (2)$$

where $L_z = L - 1$ is the length of the system in the z direction, and $x(n)$ is the exponent of the n th moment. Figures 1a, 2 and 3 show, on a log-log scale, the second, fourth and sixth moments respectively. The second moment measures the total dissipated power, and since the externally applied voltage difference is 1, it directly gives the conductance of the network. So, Figure 1a gives the scaling of the conductance as a function of L_z , giving the exponent $x(2) = 1.282(5)$. Figure 1b shows the scaling of the *variance* of the conductance distribution as a function of L_z . We see that it scales with the same exponent as the conductance itself. The same is true for the other moments. Thus, the relative fluctuations neither grow nor decrease with lattice size. The scaling of the *conductivity* with L_z is obtained by simply dividing the results for the second moment by L_z (since this is the conductance) giving $t/\nu = 2.282(5)$, where t is the conductivity exponent and ν is the correlation function exponent. Our value for t/ν is in agreement with, but more precise than, the value determined by Gingold and Lobb [17] who obtained $t/\nu = 2.276(12)$. With $\nu = 0.88$, we therefore have that $t = 2.01$. The experimental values reported for this

exponent ranges from 1.2 to 2.1 for the measurements based on microemulsions [9–13], and for the measurements based on conductor-insulator mixtures, the values 2.0 ± 0.2 [6], 1.85 ± 0.25 [7], and 1.6 ± 0.1 [8].

The exponent of the fourth moment is related to the scaling of the Nyquist noise of the random resistor network through the fluctuation-dissipation theorem as shown by Rammal *et al.* [4]. Thus, as for the second moment, the fourth moment is related to a macroscopic quantity and therefore is of direct experimental interest. However, no relation between the sixth moment of the current distribution and a directly measurable quantity has been identified. We determine $x(4) = 3.920(6)$ and $x(6) = 6.477(10)$.

If $y(n)$ is the exponent of the n th moment in the constant current ensemble, we have $\langle i^n \rangle_c \sim L_z^{y(n)}$. It is then easy to show that $y(n) = x(n) - nx(2)$. This way, we can easily change between the two ensembles. Figure 4 shows $y(n)$ as a function of n , where we see that it behaves in the classic multifractal way [5,18]: The three exponents we show do not fall on a straight line and as n increases they approach a constant that must equal $1/\nu$ [2,19]. This is shown by the dashed line in the figure. To show this relation even more clearly, we plot in Figure 5 $y(n)$ versus $1/n$, and where we use for $y(\infty)$ the best value we found for $\nu = 0.88$, [20] and references therein. The dashed line is merely to guide the eye. It connects the point at $1/n = 0$ to that at $1/n = 0.5$. We see that the exponents for the fourth and sixth moments are in agreement with this line although the sixth moment is starting to lose precision. These $y(n)$ plots demonstrate the multifractality of the current distribution in this network, but the convergence to $1/\nu$ as $n \rightarrow \infty$ is rather slow, especially when compared to the two-dimensional case [18].

The sample to sample fluctuations of the values of the conductivity (G) and the fourth moment (related the Nyquist noise strength, let us call it $K = \langle i^4 \rangle_V$) also yield interesting information about the system [21]. We have demonstrated in Figure 1b that the variance of the conductance (from sample-to-sample fluctuations) scales as the conductance itself with respect to L_z . Exactly the same behaviour is observed for the variances of the higher moments. Therefore, the distributions of $G/\langle G \rangle$ from different size systems will collapse onto

a single distribution. The same is true for $K/\langle K \rangle$. To characterize these distributions, we examined on semi-log scale these distributions against $(G - \langle G \rangle)^2 / \langle G \rangle^2$ and $(K - \langle K \rangle)^2 / \langle K \rangle^2$, respectively. Such plots should yield straight lines for Gaussian distributions. This way we found the distributions not to be normal, and a similar procedure showed them not to be lognormal. In Figures 6 and 7, we show the distributions of $G/\langle G \rangle$ and $K/\langle K \rangle$ for different lattice sizes on semi-log scale plotted against $G/\langle G \rangle$ and $K/\langle K \rangle$. For the larger values, we find in both plots straight lines which indicate exponential distributions of the form $N(G/\langle G \rangle) \sim \exp(-2G/\langle G \rangle)$ and $N(K/\langle K \rangle) \sim \exp(-1.3K/\langle K \rangle)$, respectively.

IV. CONCLUSIONS

By using a combination of efficient algorithms and a massively parallel computer, we were able to do a high precision study of the distribution and moments of currents in a three dimensional network at the percolation threshold.

Our result for the conductivity exponent is in agreement with but more precise than previous values. In addition we evaluated the exponents for the fourth (related to $1/f$ and Nyquist noise) and sixth moments. The values we have found support the notion of a multifractal current distribution for the three dimensional network.

We have furthermore studied the sample-to-sample fluctuations and the distributions of the second (conductivity) and fourth (noise) moment of the current distribution. We find that the relative fluctuations scale as the moments themselves with lattice size, and that the underlying statistical distributions appear to be exponential rather than Gaussian. Furthermore, the distribution of conductivities at the percolation threshold has proven to be an important ingredient in the formulation of scaling theories for the optical properties (ac conductivity, reflectivity, transmittivity) of two-dimensional systems such as semiconductor metal films [22] and metal-insulator composites [23]. Similar scaling theories in three dimensions, when constructed, will also need the distribution of the conductivities for three-dimensional systems at the percolation threshold, which we have presented in this paper.

ACKNOWLEDGMENTS

We thank B. Kahng, S. Roux, P. Tamayo, and B.M. Thornton for helpful discussions. We also thank Institut de Physique du Globe (Paris), GMD (Bonn), and Thinking Machines Corporation for their support through generous allocation of time on their CM5 machines.

REFERENCES

- [1] T.C. Halsey, M.H. Jensen, L.P. Kadanoff, I. Procaccia and B.I. Shraiman, Phys. Rev. A **33**, 1111 (1986).
- [2] R. Rammal, C. Tannous, P. Breton and A.M.S. Tremblay, Phys. Rev. Lett. **54** 1718 (1985)
- [3] L. de Arcangelis, S. Redner and A. Coniglio, Phys. Rev. B **31** 4725 (1985).
- [4] R. Rammal, C. Tannous and A.M.S. Tremblay, Phys. Rev. A **31** 2662 (1985).
- [5] L. de Arcangelis, S. Redner and A. Coniglio, Phys. Rev. B **34**, 4656 (1986).
- [6] S.I. Lee, Y. Song, T.W. Noh, X.D. Chen and J.R. Gaines, Phys. Rev. B **34**, 6719 (1986).
- [7] Y. Song, T.W. Noh, S.I. Lee and J.R. Gaines, Phys. Rev. B **33**, 904 (1986).
- [8] M. Rohde and H. Micklitz, Phys. Rev. B **36**, 7289 (1987).
- [9] M. Laguës, J. Physique Lett. **40**, L331 (1979).
- [10] M. Laguës and C. Sauterey, J. Phys. Chem. **84**, 3503 (1980).
- [11] S. Bhattacharya, J.P. Stokes, M.W. Klein and J.S. Huang, Phys. Rev. Lett. **55**, 1884 (1985).
- [12] H.F. Eicke, R. Hilfiker and H. Thomas, Chem. Phys. Lett. **125**, 295 (1986).
- [13] M.T. Clarkson, Phys. Rev. A **37**, 2079 (1988).
- [14] D. Stauffer, J. Adler and A. Aharony, J. Phys. A **27** L475 (1994).
- [15] G.G. Batrouni and A. Hansen, J. Stat. Phys. **52** 747 (1988).
- [16] C.H. Tong, *A Comparative Study of Preconditioned Lanczos Methods for Non-symmetric Linear Systems*, Sandia Technical Report SAND91-8240 (1992).
- [17] D.B. Gingold and C.J. Lobb, Phys. Rev. B **42** 8220 (1990).

- [18] For a review of the multifractal properties of the current distribution in random resistor networks, see *e.g.* A. Hansen in *Statistical Models for the Fracture of Brittle Materials*, edited by H.J. Herrmann and S. Roux (North-Holland, Amsterdam, 1990).
- [19] G.G. Batrouni, A. Hansen and M. Nelkin, *J. Physique* **48**, 771 (1987).
- [20] J. Adler, Y. Meir, A. Aharony and A.B. Harris, *Phys. Rev. B* **41**, 9183 (1990).
- [21] A.B. Harris, Y. Meir and A. Aharony, *Phys. Rev. B* **41**, 4610 (1990).
- [22] Y. Yagil, M. Yosefin, D.J. Bergman and G. Deutscher, *Phys. Rev. B* **43** 11342 (1991).
- [23] T.W. Noh, P.H. Song, S.-I. Lee, D.C. Harris, J.R. Gains and J.C. Garland, *Phys. Rev. B* **46** 4212 (1992).

FIGURES

FIG. 1. a) The second moment of the current (*i.e.* the conductance G) scales as a power of the system size L_z , with an exponent equal to $-1.282(5)$. b) The variance of the conductance distribution scales exactly as the conductance itself with the system size, L_z .

FIG. 2. Power law scaling of the fourth moment as a function of the system size L_z . The exponent is $-3.920(6)$.

FIG. 3. Power law scaling of the sixth moment as a function of the system size L_z . The exponent is $-6.477(10)$.

FIG. 4. $y(n)$, the exponent of the n th moment in the constant current ensemble, as a function of n . As n increases, $y(n)$ approaches the dashed line which is given by $1/\nu$.

FIG. 5. Same as Figure 4, but shows $y(n)$ as a function of $1/n$. This shows very clearly that as $n \rightarrow \infty$, $y(n) \rightarrow 1/\nu$. The dashed line is a guide to the eye and simply connects the points at $1/n = 0$ and $1/n = 0.5$.

FIG. 6. Histogram of $G/\langle G \rangle$ on semilog scale. It shows that the distribution for larger values of $G/\langle G \rangle$ is exponential.

FIG. 7. Histogram of $K/\langle K \rangle$ on semilog scale. It shows that the distribution for larger values of $K/\langle K \rangle$ is exponential.

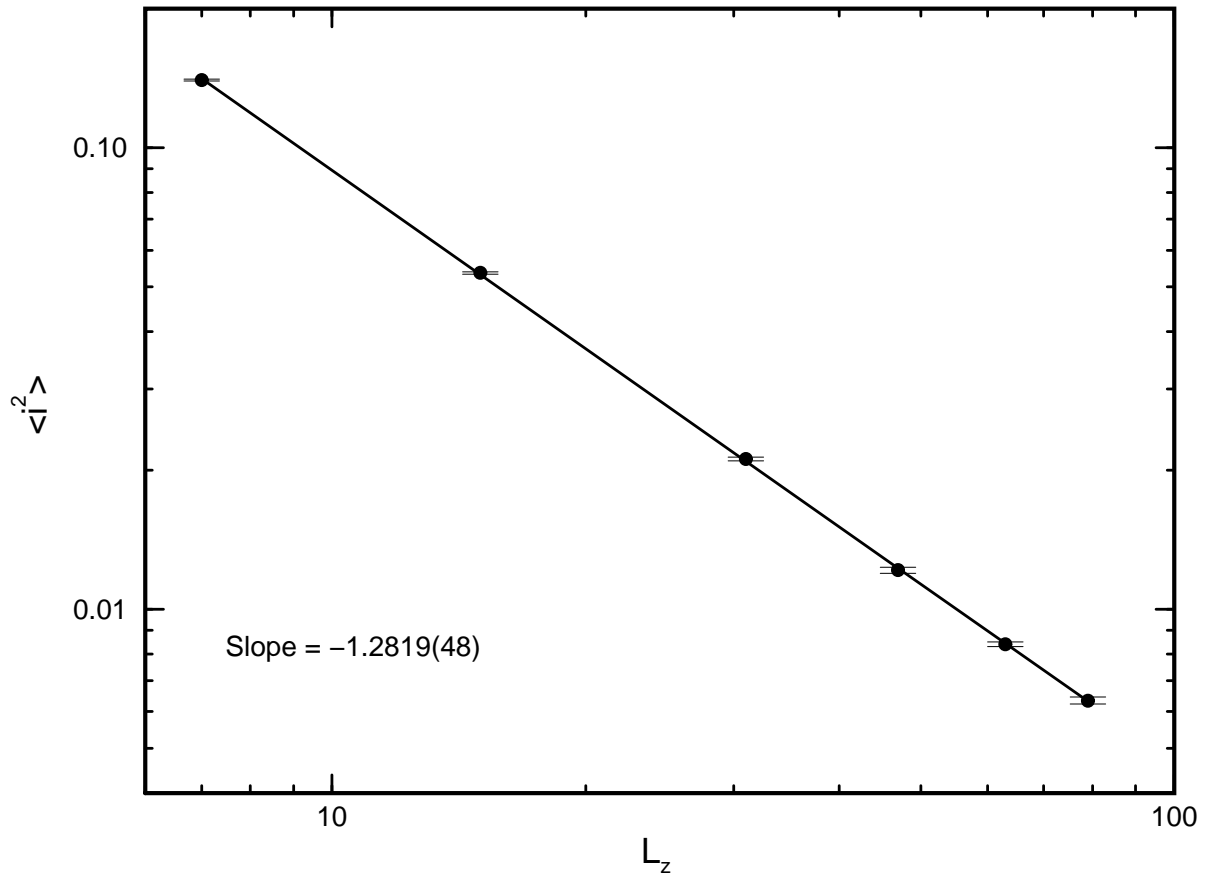


Figure 1a

G.G. Batrouni, A. Hansen and B. Larson

“Current Distribution in the 3D Random Resistor Network”

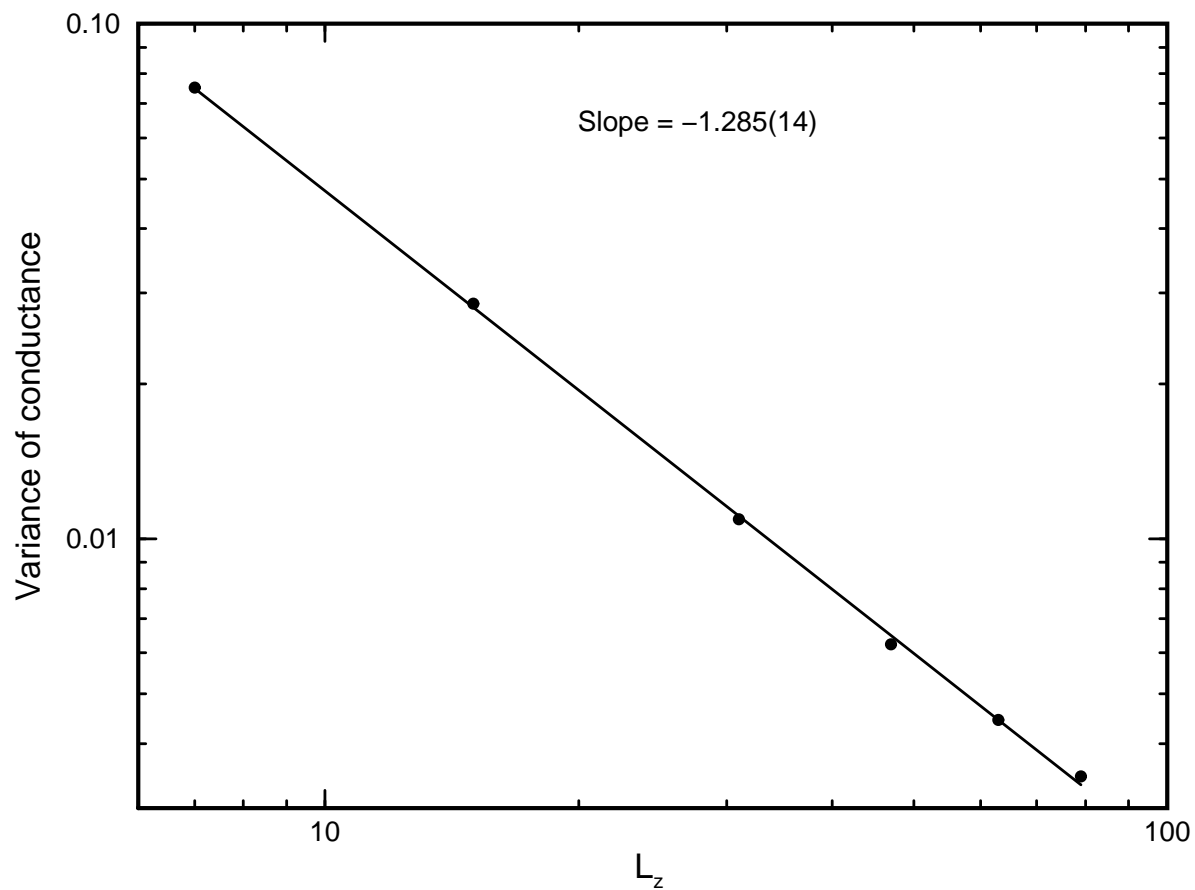


Figure 1b

G.G. Batrouni, A. Hansen and B. Larson

“Current Distribution in the 3D Random Resistor Network”

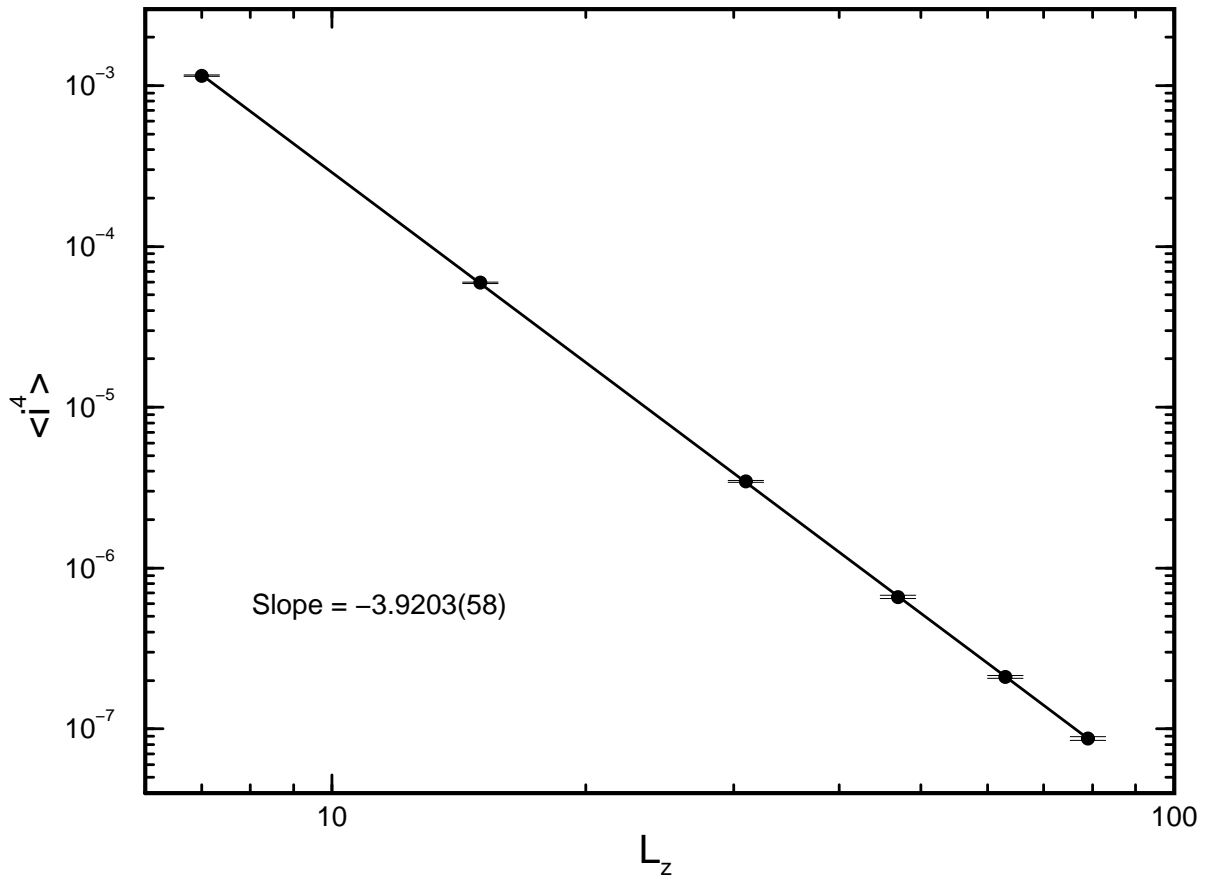


Figure 2

G.G. Batrouni, A. Hansen and B. Larson

“Current Distribution in the 3D Random Resistor Network”

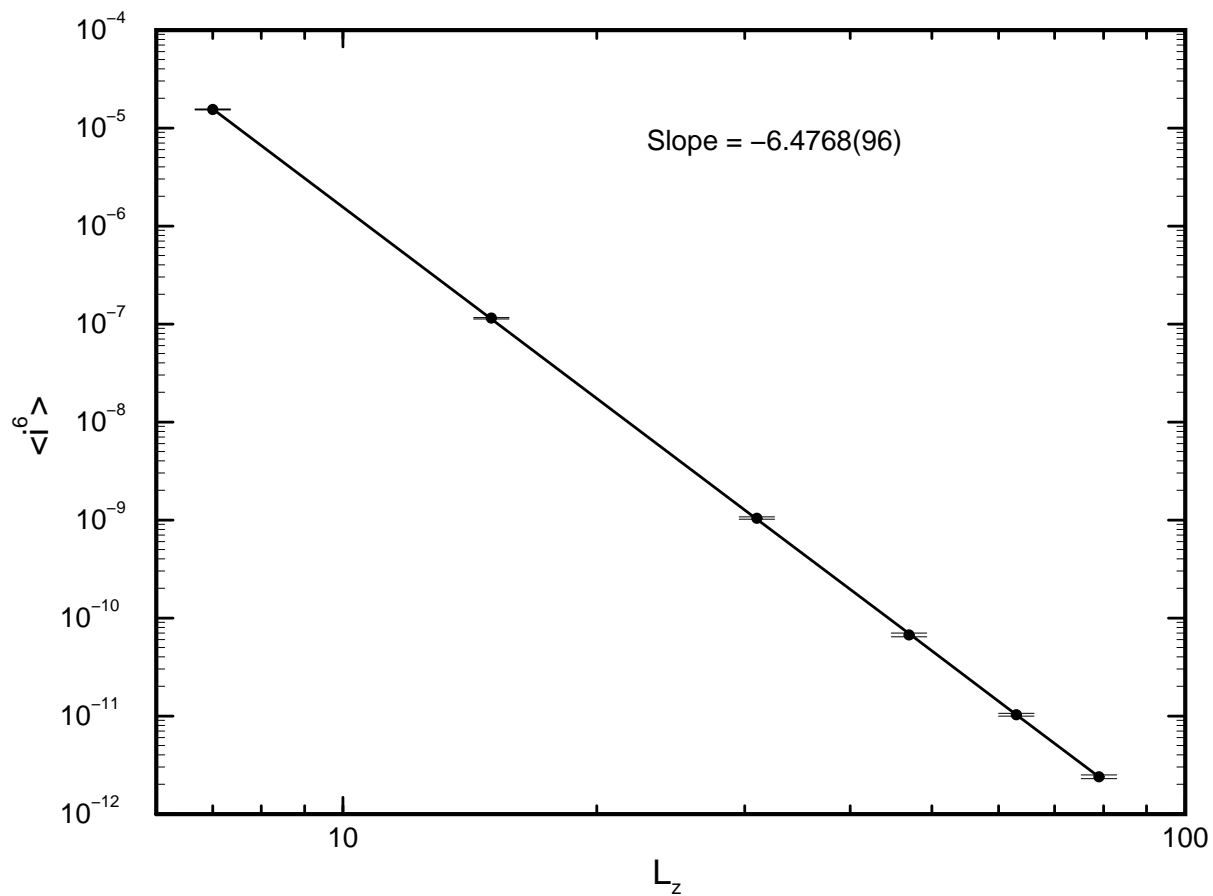


Figure 3

G.G. Batrouni, A. Hansen and B. Larson

“Current Distribution in the 3D Random Resistor Network”

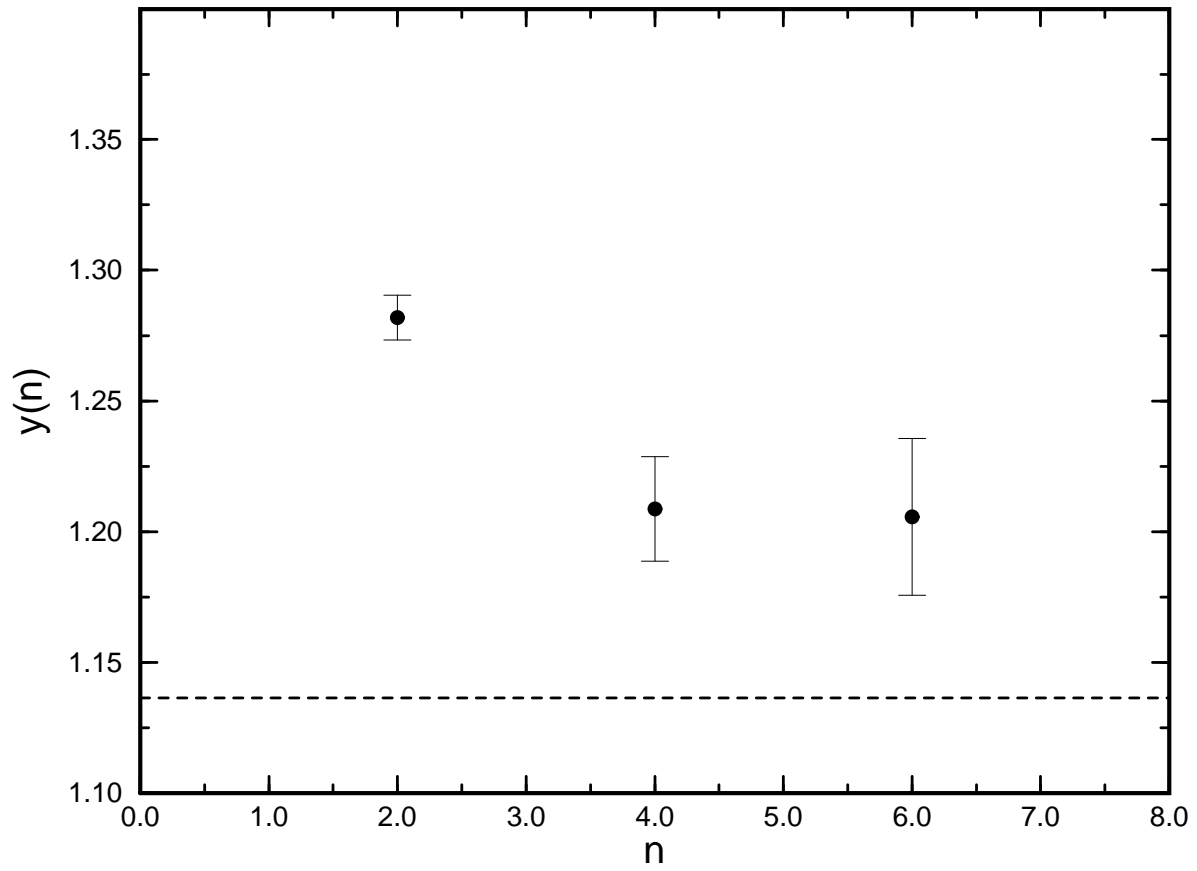


Figure 4

G.G. Batrouni, A. Hansen and B. Larson

“Current Distribution in the 3D Random Resistor Network”

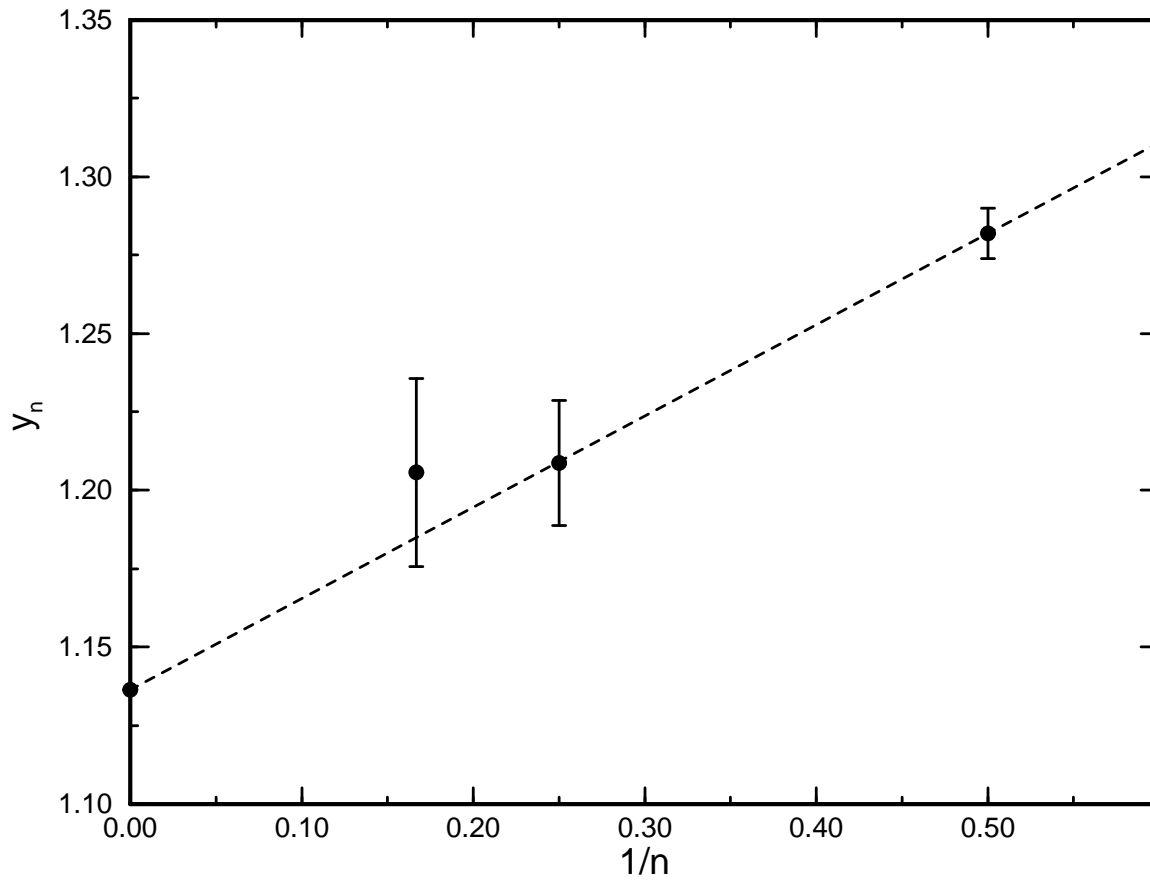


Figure 5

G.G. Batrouni, A. Hansen and B. Larson

“Current Distribution in the 3D Random Resistor Network”

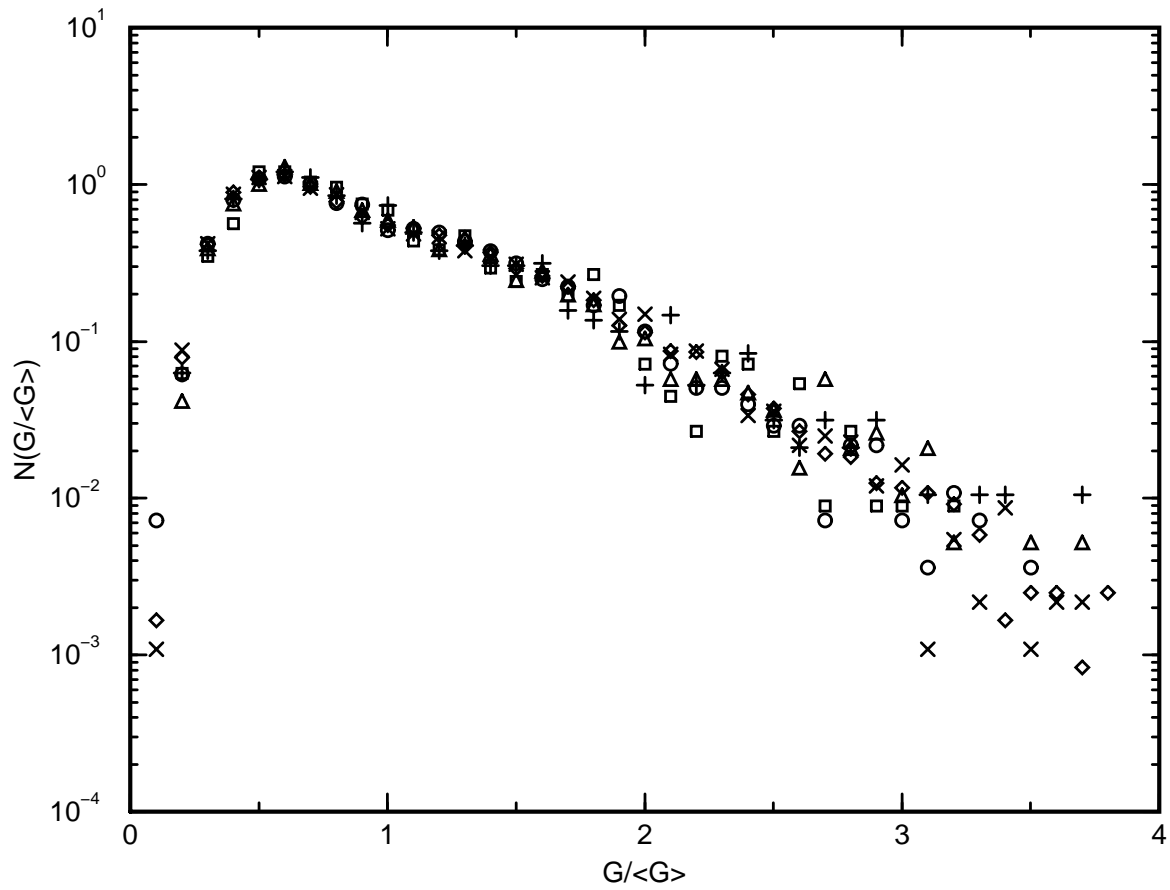


Figure 6

G.G. Batrouni, A. Hansen and B. Larson

“Current Distribution in the 3D Random Resistor Network”

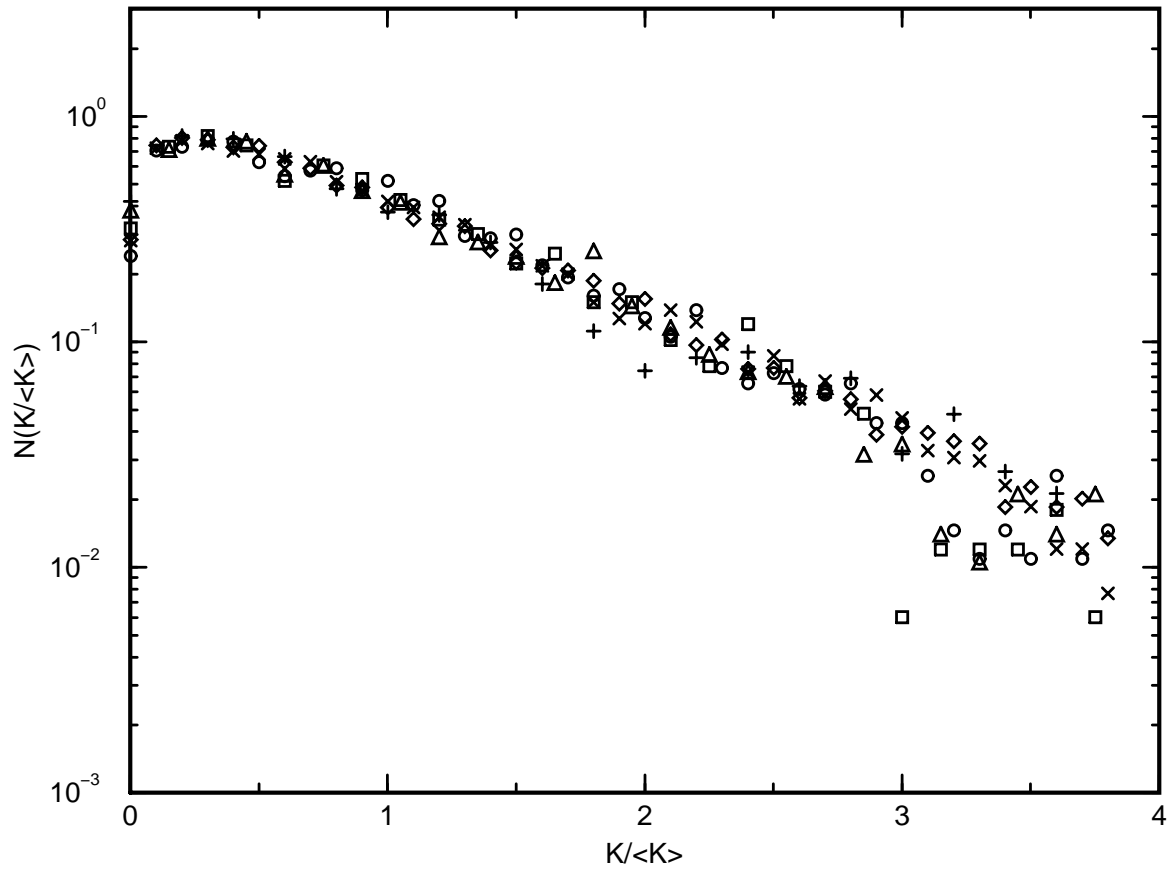


Figure 7

G.G. Batrouni, A. Hansen and B. Larson

“Current Distribution in the 3D Random Resistor Network”